pH-Responsive Amphoteric p (APTMACl-co-AMPS) Hydrogel as Effective Multiple Dye Sponge Network From Aqueous Media

Sahin Demirci[1], Betul Ari[1], Nahit Aktas[2,3] and Nurettin Sahiner[1,4,5]*

[1]Canakkale Onsekiz Mart University, Faculty of Science and Arts, Department of Chemistry, and Nanoscience, Technology Research and Application Center (NATRAC), Canakkale, Turkey, [2]Engineering Faculty, Department of Chemical Engineering, Campus, Van Yüzüncü Yil University, Van, Turkey, [3]Faculty of Engineering, Department of Chemical Engineering, Kyrgyz-Turkish Manas University, Bishkek, Kyrgyzstan, [4]Department of Chemical and Biomolecular Engineering, University of South Florida, Tampa, FL, United States, [5]Department of Ophthalmology, Morsani College of Medicine, University of South Florida, Tampa, FL, United States

Here, the cationic poly (3-acrylamidepropyl trimethyl ammonium chloride) [p (APTMACl)], anionic poly (2-acrylamido-2methylpropane sulfonic acid) [p (AMPS)], and amphoteric poly (APTMACl-co-AMPS) hydrogels were prepared *via* free-radical polymerization techniques as pH-sensitive hydrogels. The prepared systems were used in methylene blue (MB), and Eosin Y (EY) removal from aqueous media. HCl-treated p (APTMACl-co-AMPS) hydrogels prepared in 1:3 mol ratio adsorbed higher amount of MB and EY from their corresponding 50 ml 50 ppm aqueous solutions that are 47.5 ± 0.9, and 10.7 ± 0.1 mg/g, respectively. Also, the adsorbed amount of MB and EY by HCl-treated p (APTMACl-co-AMPS) hydrogels decreased with the increase in the medium pH from 3.0 to 9.0. It was also observed that HCl-treated p (APTMACl-co-AMPS)-3 hydrogels removed 39.2 ± 0.2, and 28.1 ± 1.0 mg/g MB and EY dyes simultaneously from their corresponding 50 ml 50 ppm aqueous mixture solutions. MB and EY adsorption by HCl-treated p (APTMACl-co-AMPS)-3 hydrogels were found to abide by pseudo-first-order adsorption kinetics. Moreover, MB adsorption by HCl-treated p (APTMACl-co-AMPS) hydrogels were found to fit with Freundlich, EY adsorption fit with Langmuir isotherms. The distribution coefficient values of HCl-treated p (APTMACl-co-AMPS) hydrogels were calculated as 3.7 ± 0.1 and 1.3 ± 0.1 for MB and EY, respectively. The calculated selectivity coefficient value showed that HCl-treated p (APTMACl-co-AMPS) hydrogels are at least 3-fold higher selective to MB than EY.

Keywords: dye removal, pH sensitive hydrogels, amphoteric hydrogel, multiple dye removal, p(APTMACl-co-AMPS) hydrogels

1 INTRODUCTION

Water is eventually contaminated with undesired contaminants that might be hazardous to living organisms, due to it is being the main solvent and is utilized in industrial, agricultural, or home activities (Anjaneyulu et al., 2005; Hai et al., 2007; Crini and Lichtfouse, 2019). Additionally, the contamination of water is becoming more prevalent and diverse as a result of a variety of factors, including industrial waste, mining operations, chemical fertilizers, pesticides, and urban growth

(Anjaneyulu et al., 2005; Hai et al., 2007). Undeniably, chemical-related water contamination has become a serious concern and priority for both society and governmental authorities, but more crucially for the whole human beings (Sharma and Sanghi, 2012; Rathoure and Dhatwalia, 2016). A sustained effort to protect water resources is critical in this context (Leverenz and Asano, 2011; Saravanane et al., 2014). Over the last 30 years, some of the most common methods used to protect the clean water resources and/or to attain clean/reusable water from polluted waters, flotation, precipitation, oxidation, solvent extraction, evaporation, adsorption, ion exchange, membrane filtration, electrochemistry, biodegradation, phytoremediation, and biological technologies are being used prominently (Katheresan et al., 2018; Salgot and Folch, 2018; Crini and Lichtfouse, 2019; Cao et al., 2021; Cao et al., 2022).

Synthetic dyes, which are widely utilized in the leather, paper, and textile sectors and are expected to create 700,000 tons of diverse colorants from around 100,000 commercially available colors each year, are among the most dangerous water pollutants (Gupta and Suhas, 2009; Rafatullah et al., 2010; Abdi et al., 2017; Wagner et al., 2020). Toxic dyes are frequently discarded into environmental waterways after they are used. It has been reported that the textile industry alone releases more than half of the existing dye wastes (54%) as seen in the environment around the world, and the textile industry is followed by the dyeing industry (21%), the paper and pulp industry (10%), the tannery and dye industry (8%), and the paint manufacturing industry (7%) (De Gisi et al., 2016; Mojsov et al., 2016). Although the actual amount of paint waste released into the environment by each business is unknown, it is safe to say that the number that will cause a significant environmental problem is fairly substantial (Dargahi et al., 2018; Gan et al., 2018).

Hydrogels as soft materials have attracted great attention due to their unique and interesting properties (Das et al., 2016; Das et al., 2017; Okesola and Smith, 2016). The water uptake and swelling ability of hydrogels make them promising materials in wastewater treatment employing adsorption techniques (Sahiner, 2013). In recent years, hydrogels were prepared in various shapes and formulations (cylindric, film, etc.), ionic character (anionic, cationic, or amphoteric), and size (nano, micro, or macro) were successfully used in the removal of pollutants from aqueous media (Say et al., 2004; El-Hamshary et al., 2007; Yildiz et al., 2014; Sartape et al., 2017; Van Tran et al., 2018; Kubilay et al., 2021). A variety of pollutants of ionic nature be readily be removed from aqueous media can be handled by utilization of hydrogels as adsorbents (Sahiner, 2013).

Here, the preparation cationic p (APTMACl), anionic p (AMPS), and amphoteric p (APTMACl-co-AMPS) hydrogels were reported via free radical polymerization, and then they were used in the removal of MB and EY dyes from their corresponding aqueous solutions. The effect of ionic nature, acid/base treatment of the adsorbents, the pH of dye solutions, and the effect of the dye concentrations on the removal of the related dyes from aqueous medium by the hydrogels were investigated. Moreover, the adsorption kinetics and adsorption isotherms for MB and EY adsorption by amphoteric hydrogel were investigated by applying pseudo-first and second order

kinetic models, Langmuir, Freundlich, Temkin, and Dubinin-Radushkevic isotherms. Furthermore, the simultaneous removals of both MB and EY from their corresponding mixture solutions were also carried into amphoteric hydrogels and important parameters such as distribution and selectivity coefficients were determined.

2 EXPERIMENTAL

2.1 Materials
2-acrylamido-2-methyl-1-propane sulfonic acid sodium salt (AMPS, 50 wt% in H_2O, Sigma-Aldrich, St. Louis, MO, United States) and (3-acrylamidopropyl)trimethyl ammonium chloride (APTMACl, 75 wt% in H_2O, Sigma-Aldrich, Tokyo, Japan) as monomers, N, N′-methylenebis (acrylamide) (MBA, 99%, Sigma–Aldrich, St. Louis, MO, United States) as a crosslinker, tetramethylethylenediamine (TEMED, 98%, Merck, Darmstadt, Germany) as an accelerator, ammonium persulfate (APS, 99%, Sigma–Aldrich, Germany) as initiator were used in cationic p (APTMACl), anionic p (AMPS), and amphoteric p (APTMACl-co-AMPS) hydrogel preparation. Methylene blue hydrate (MB, Sigma–Aldrich, 97%, India), Eosin Y disodium salt (EY, ≥ 90%, Sigma–Aldrich, St. Louis, MO, United States), and methyl orange (MO, Fluka, Poland) were used as dye sources. Hydrochloric acid (HCl, 37%, Carlo Erba, France), and sodium hydroxide (NaOH, pellets extra pure, AFG Bioscience, United States) were used in the acid/base treatment of the hydrogels. Sodium phosphate monobasic (≥99%, Sigma-Aldrich, St. Louis, MO, United States) was used for the preparation of buffer solutions. All aqueous solutions were prepared by using distilled water (DI, GFL 2108 water distiller, Germany).

2.2 pH-Sensitive Cationic, Anionic, and Amphoteric Hydrogels
The preparation of cationic p (APTMACl), anionic p (AMPS), and amphoteric p (APTMACl-co-AMPS) hydrogels were carried out via simultaneous free-radical polymerization and crosslinking reaction with some modification according to the earlier report (Seven and Sahiner, 2013; Sahiner and Seven, 2015). To synthesize the cationic p (APTMACl) hydrogel, 3.264 ml of APTMACl was added to 1.684 ml of DI water and stirred at 500 rpm for 30 min at room temperature. Then, 1% mole MBA (according to mole of monomer, 20.4 mg) crosslinker and 10 μL of TEMED were added to this mixture and stirred at 500 rpm until a homogeneous mixture was obtained. Finally, 1% mole initiator APS solution in 1 ml DI water (according to mole of monomer, 30.59 mg/ml) was added to this solution, and the solution was immediately transferred into a 4 mm diameter plastic pipettes and kept at room temperature for 2 h for polymerization and crosslinking. Next, the obtained hydrogels were cut to about the same dimensions (approximately 6 mm in length) and washed 5 times with DI water to get rid of impurities and unreacted chemicals. The washed hydrogels were then dried in an oven at 50°C and saved in a zipper storage bag for later use. To synthesize the anionic p (AMPS) hydrogel, 0.0131mol of AMPS

monomer, and 1% moles of crosslinker MBA (according to the mole of monomer, 20.4 mg) and 10 μL of TEMED were placed in a glass vial and mixed at 500 rpm until a homogeneous mixture was obtained at room temperature. To start the polymerization, 1% mole APS solution in 1 ml water (according to mole of monomer, 30.59 mg/ml) initiator was added to this solution, and the solution was quickly transferred into a 4 mm diameter plastic pipettes. The above steps were followed for polymerization, wash, dry, and storage of the prepared p (AMPS) hydrogels.

Amphoteric p (APTMACl-co-AMPS) hydrogels were synthesized using APTMACl:AMPS monomer mix at various mole ratios e.g., 3:1, 1:1, 1:3, respectively. For this purpose, the APTMACl:AMPS solution was placed into a glass vial at these ratios, and total moles of monomers were kept in 0.01314 mol. The MBA crosslinker, 1% mole of the total mole of monomers, and 10 μL of TEMED were also added to the monomer mix solutions, separately. Finally, 1% mole of initiator APS (30.59 mg/ml) based on the total mole of both monomers was added to the hydrogel precursor solution and was rapidly transferred to 4 mm diameter plastic pipettes. The same steps as above were followed for polymerization, washing, drying, and storage conditions. The prepared amphoteric p (APTMACl-co-AMPS) hydrogels at mole ratio of 3:1, 1:1, and 1:3 was labelled as p (APTMACl-co-AMPS)-1, p (APTMACl-co-AMPS)-2, and p (APTMACl-co-AMPS)-3, respectively.

Also, to increase the acidity or basicity of the amphoteric p (APTMACl-co-AMPS) hydrogels, approximately 1 g of the hydrogel was treated with aqueous solutions of 250 ml 1 M HCl and 250 ml 1 M NaOH for 12 h, separately. HCl and NaOH treated amphoteric p (APTMACl-co-AMPS) hydrogels were washed with DI water for 30 min and dried in an oven at 50°C. It was stored in zip lock bags to be used in absorption studies.

2.3 Swelling Properties of Hydrogels

The swelling ratio (%SR) of all hydrogels was performed in DI water. About 30 mg of each piece of dry hydrogel was allowed to swell in 30 ml of DI water to determine the SR%. The hydrogel pieces were taken from the DI water at certain time intervals and surface water was removed with filter paper. Then, hydrogel pieces were weighed and placed back into the same medium and continued to swell until the swelling equilibrium was reached. The SR% of hydrogels was calculated using **Eq. 1**.

$$SR\% = [(m_t - m_{t0})/m_{t0}] \times 100 \qquad (1)$$

Here, "m_t" is the weight of the swollen hydrogel at time t, "m_{t0}" is the initial weight of the dry hydrogels.

Equilibrium swelling values of all amphoteric hydrogels at different pH conditions were obtained by allowing a 30 mg hydrogel piece immersed in 30 ml of prepared 500 mM sodium phosphate buffer solution at different pHs varying between 3.0 and 9.0. After about 8 h, the SR% values of amphoteric hydrogels at different pHs were calculated using **Eq. 1**. The pHs of buffer solutions was adjusted with the addition of 1 M HCl and 1 M NaOH solutions. All studies were performed in triplicate and SR% values were given as average with the standard deviations.

2.4 Adsorption Experiment From Aqueous Medium With Hydrogels

The prepared pH-sensitive cationic p (APTMACl), anionic p (AMPS), and amphoteric p (APTMACl-co-AMPS) hydrogels were used for the removal of some organic dyes from the aqueous medium. Methylene blue (MB) was used as a cationic dye, and methyl orange (MO), eosin Y (EY) were used as anionic dyes in adsorption studies. In brief, certain amounts of prepared hydrogels, ~50 mg was placed in 50 ml of 50 ppm dye solutions and stirred for 8 h at 300 rpm mixing rate. The adsorbed amounts of dyes were determined by UV-Vis spectrometer from prepared calibration curves of related dyes at 664 nm for MB, 464 nm for MO, and 515 nm for EY, respectively. The effect of the amount of adsorbent and pH on adsorption studies were carried out with MB and EY *via* using p (APTMACl-co-AMPS)-3 hydrogels. All the measurements were performed in triplicate and results were given as average with standard deviations.

2.5 Adsorption Kinetics, Isotherms, and Important Parameters for Dye Removal With pH-Sensitive Amphoteric Hydrogels

2.5.1 Adsorption Kinetics

The two most used, and well-known kinetic models, pseudo-first order and pseudo-second order models were applied in dye absorption studies to identify the rate and mechanism of absorption of dyes (Kubilay et al., 2021). The equations of pseudo-first order and pseudo-second order models in **Eq. 2**, and **Eq. 3** was followed:

$$\ln(q_e - q_t) = \ln(K_1 q_e) - K_1 t \qquad (2)$$

$$t/q_t = 1/(K_2 q_e 2) + t/q_e \qquad (3)$$

where; "q_e" is the absorbed amount of molecule at equilibrium (mg. g^{-1}), "q_t" is the absorbed amount of molecule at time t (mg.g^{-1}), K_1 is the rate constant for the pseudo-first-order model (min^{-1}), and K_2 is the rate constant for the pseudo-second-order model (g.mg^{-1}. min^{-1}).

2.5.2 Adsorption Isotherms

According to the Langmuir model, it was assumed that the adsorption energy is uniform and there is no adsorbate migration in the surface plane (Kubilay et al., 2021), and is expressed as in **Eq. 4**:

$$C_e/q_e = 1/q_m K_L + C_e/q_m \qquad (4)$$

where, "q_e" is the amount of solute adsorbed per unit weight of adsorbent at equilibrium (mg.g^{-1}), "C_e" is the equilibrium concentration of the solute in bulk solution (mg.L^{-1}), "q_m" is the maximum adsorption capacity (mg.g^{-1}), and K_L is the Langmuir constant (L.mg^{-1}).

The Freundlich isotherm assumes heterogeneous surface energies and it becomes more heterogeneous as the value of the slope approaches zero (Kubilay et al., 2021). Freundlich equation can be also written as **Eq. 5**:

$$\ln q_e = \ln K_F + (1/n) \ln C_e \qquad (5)$$

where, "K_F" is a constant indicative of the relative adsorption capacity of the adsorbent ($mg^{1-(1/n)} L^{1/n} \cdot g^{-1}$) and "$n$" is a constant indicative of the intensity of the adsorption, and "C_e" is the equilibrium concentration of the solute in bulk solution ($mg.L^{-1}$).

According to the Temkin model, it was assumed that the adsorption heat of all molecules in the layer decreases linearly with the coverage area due to the adsorbent-adsorbate interactions and the adsorption is characterized by a homogeneous distribution of binding energies up to a maximum binding energy (Kubilay et al., 2021). The equation can be written as follows **Eq. 6**:

$$q_e = RT/b \ln K_T + RT/b \ln C_e \qquad (6)$$

where "q_e" is the amount of solute adsorbed per unit weight of adsorbent at equilibrium ($mg.g^{-1}$), "$RT/b = B$," "R" is the gas constant ($8.314 \, J \, mol^{-1}.K^{-1}$), "$T$" is the absolute temperature in Kelvin unit, "b" is related to the heat of adsorption ($J.mol^{-1}$), "K_T" is the Temkin constant ($L.mg^{-1}$), and "C_e" the equilibrium concentration of the solute in bulk solution ($mg.L^{-1}$).

Dubinin-Radushkevich isotherm model is generally applied to express the adsorption mechanism on heterogeneous surfaces (Kubilay et al., 2021). It is expressed by **Eq. 7**:

$$\ln q_e = \ln q_m - B\varepsilon^2 \qquad (7)$$

where "q_m" represents the adsorption capacity ($mg.g^{-1}$), "R" is the gas constant ($8.314 \, J \, mol^{-1}.K^{-1}$), and "$T$" refers to the temperature as Kelvin. In addition, ε^2 value is given by $\varepsilon^2 = [RT \ln (1 + 1/Ce)]^2$ equation.

2.5.3 Distribution, and Selectivity Coefficients

The well-known and important coefficients of distribution and selectivity in adsorption studies of MB and EY dyes in 50 ml, 25, 50, and 100 ppm solutions using HCl-treated p (APTMACl-co-AMPS)-3 hydrogels were calculated by employing **Eqs 8**, **9**, respectively:

$$K_d = (q_e.C_e^{-1}) (\text{amount of hydrogel in g})$$
$$\cdot (\text{volume of solution in L})^{-1} \qquad (8)$$

$$k = (K_d (MB)) \cdot (K_d (EY))^{-1} \text{ and } k = (K_d (EY)) \cdot (K_d (MB))^{-1} \qquad (9)$$

where "K_d" and "k" are the distribution and selectivity coefficients for MB or EY dyes, respectively, while "q_e" is the amounts of adsorbate per unit weight of adsorbent ($mg.g^{-1}$) and "C_e" denotes the equilibrium concentration of a given solute in the bulk solution (ppm) of MB or EY dyes.

3 RESULTS AND DISCUSSION

3.1 Synthesis of Cationic, Anionic, and Amphoteric Hydrogels

The preparations of cationic, anionic, and amphoteric hydrogels were accomplished by simultaneous free-radical polymerization and crosslinking reaction. The schematic presentations of hydrogel preparation were given in **Figure 1A**. The prepared p (APTMACl) hydrogels are cationic due to ammonium chloride, and p (AMPS) hydrogels are anionic due to sulfonic acid groups in their monomers, respectively. On the other hand, the p (APTMACl-co-AMPS) hydrogels in the various ratio of monomers are amphoteric due to the presence of this cationic ammonium chloride, and anionic sulfonic acid groups. The prepared p (APTMACl-co-AMPS) hydrogels using APTMACl: AMPS monomer mix at various mole ratios e.g., 3:1, 1:1, and 1:3, were denoted as p (APTMACl-co-AMPS)-1, p (APTMACl-co-AMPS)-2, and p (APTMACl-co-AMPS)-3, respectively.

In **Figure 1B**, the digital camera images of all hydrogels in both dry and swollen forms were shown on a plate with 30 mm diameter. It can be clearly seen that the colors of dry hydrogels are different from each other. The color of dry p (APTMACl) hydrogels is brownish, and dry p (AMPS) hydrogels are light yellow-transparent. Similarly, the color of amphoteric hydrogels changed from brownish to clear transmit with the decreasing ratio of APTMACl monomers. It is clearly seen that the swollen hydrogels differ in their dimensions according to the APTMACl:AMPS ratio. The sizes of swollen p (APTMACl-co-AMPS)-1 and p (APTMACl-co-AMPS)-3 hydrogels are almost similar and bigger than the size of swollen p (APTMACl-co-AMPS)-2 hydrogels. This could be due to neutralization of charges as equal amounts of anionic and cationic monomer is used. As can be seen from digital camera images of p (APTMACl-co-AMPS) hydrogels, the used APTMACl:AMPS monomer mix ratio to prepare amphoteric hydrogels directly affect the swelling ability of hydrogels. The swelling properties of prepared cationic p (APTMACl), anionic p (AMPS), and amphoteric p (APTMACl-co-AMPS)-1, p (APTMACl-co-AMPS)-2, and p (APTMACl-co-AMPS)-3 hydrogels were studied in detail and mentioned in **Section 3.2**.

Fourier Transform Infrared Radiation (FT-IR, Perkin Elmer, Spectrum100, Perkin Elmer Instruments, Norwalk, CT, United States) spectrophotometer was used to characterize the functional groups, e.g., anionic, cationic, and amphoteric hydrogel samples. All spectra were recorded at $4 \, cm^{-1}$ resolutions using the ATR technique in the scanning range from 4,000 to $650 \, cm^{-1}$ with a total of 4 scans. It was clearly shown in **Figure 2A**, the cationic p (APTMACl) hydrogels and anionic p (AMPS) hydrogels possess their characteristic peaks, whereas the amphoteric hydrogels possessed the same peaks from both cationic and anionic monomers as expected. In brief, at about 3,320 and $3,280 \, cm^{-1}$ the NH_2 stretching peaks, and at $1,650 \, cm^{-1}$ the C=O stretching peak from amide groups were observed for all samples. On the other hand, at $1,628 \, cm^{-1}$ the quaternary ammonia peaks from FT-IR spectrum of p (APTMACl) hydrogels, and asymmetric and symmetric stretching peaks of O-S-O and stretching peaks of S=O were also observed at 1,306, 1,183, and $1,046 \, cm^{-1}$, respectively for p (AMPS) were observed. Moreover, the intensity decreasing on C-N stretching peaks at 969, and $917 \, cm^{-1}$ with decreasing of ratios of APTMACl, and intensity increasing on S-O asymmetric bending peaks at $1,306 \, cm^{-1}$ with increasing of the ratio of AMPS on FT-IR spectra of amphoteric hydrogels were also clearly confirmed the successful syntheses of the amphoteric hydrogels.

FIGURE 1 | (A) the schematic presentation of the preparation, and **(B)** digital camera images of cationic p (APTMACl), anionic p (AMPS), and amphoteric p (APTMACl-co-AMPS)-1, p (APTMACl-co-AMPS)-2, and p (APTMACl-co-AMPS)-3 hydrogels.
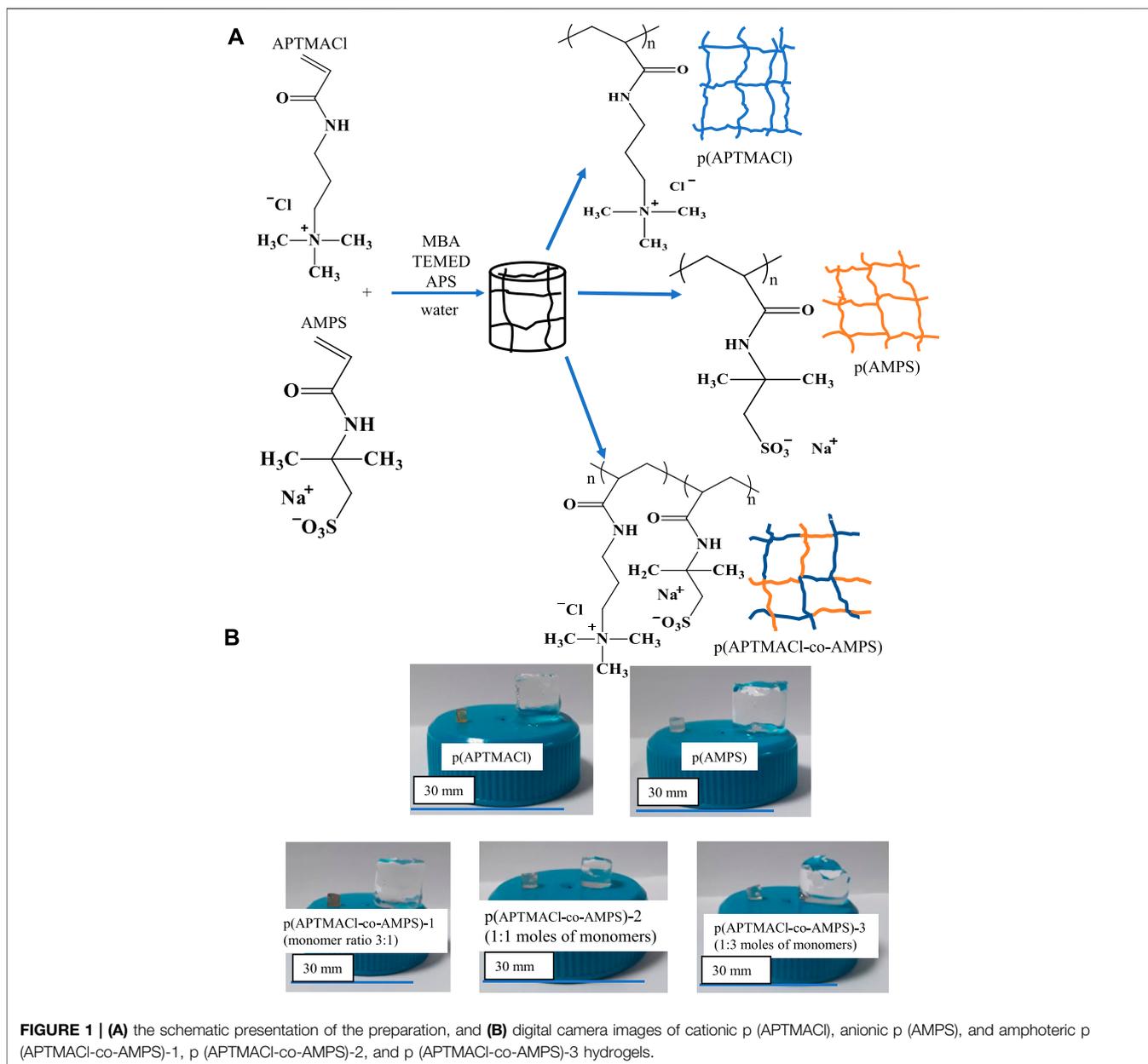
Thermal stability of anionic, cationic, and amphoteric hydrogel samples was characterized *via* Thermogravimetric Analyzer (TGA, SII TG/DTA6300, Exstar, Seiko Ins. Corp, Chiba, Japan), About 3 mg hydrogel piece was put in the sample pan and the furnace was heated to 100°C to remove humid that existed in all the hydrogel piece. Thermogravimetric analysis of the samples, which were dehumidified, was performed by heating the hydrogel samples from 90 to 700°C under 10°C/min heating rate and a nitrogen flow of 200 ml/min. In **Figure 2B**, thermal decomposition thermogram of p (APTMACl), p (AMPS), p (APTMACl-co-AMPS)-1, p (APTMACl-co-AMPS)-2, and p (APTMACl-co-AMPS)-3 hydrogels were illustrated. In **Figure 2B**, similar three-step thermal decomposition patterns were observed for all the p (AMPS)

and p (APTMACl-co-AMPS)-3 hydrogels. The first stage of thermal decomposition for p (AMPS) and p (APTMACl-co-AMPS)-3 hydrogels started with a weight loss of 7.6 and 5.2% between 127–290°C with a weight loss associated with the moisture content of the hydrogels. Thermal decomposition continued between 290–330°C with weight losses of 38 and 50%, respectively. The final step of thermal decomposition resulted in a cumulative weight loss of 92 and 90% at 700°C, respectively. On the other hand, similar three-step thermal degradation profiles were observed for, p (APTMACl-co-AMPS)-1, p (APTMACl-co-AMPS)-2, p (APTMACl-co-AMPS)-3 hydrogels. The initial decomposition steps of these hydrogels were started in the range of 170–330°C with a weight loss of 18, 11, and 3%, respectively. The second decomposition
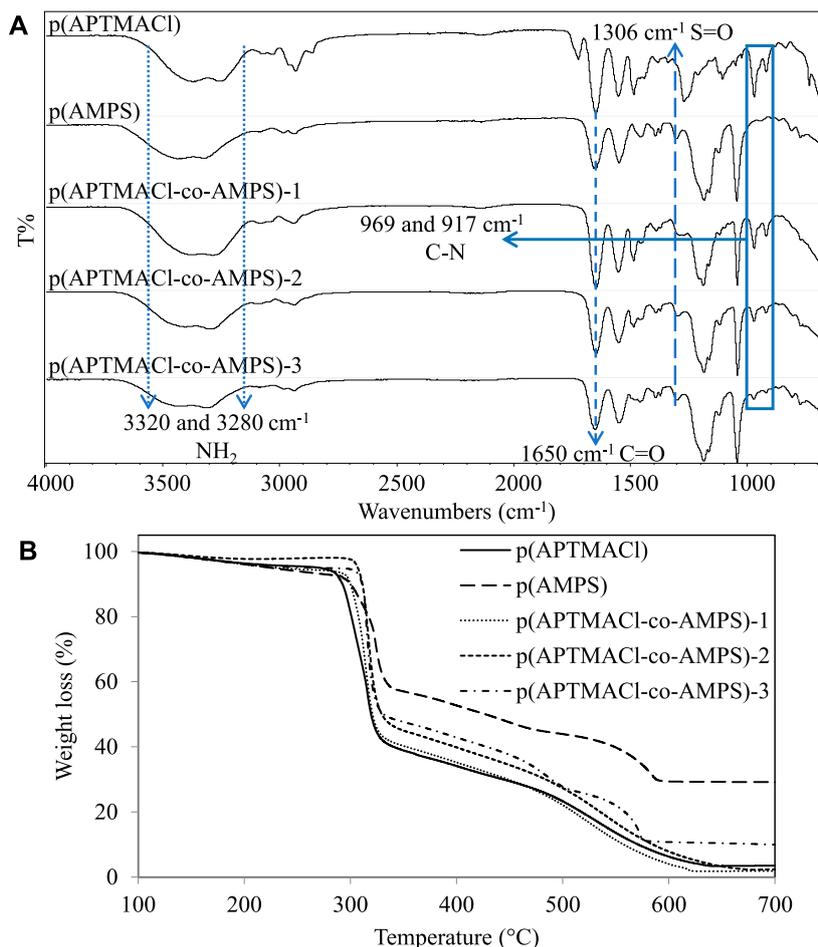
FIGURE 2 | (A) FT-IR spectra and **(B)** thermal decomposition curves of p (APTMACl), p (AMPS), p (APTMACl-co-AMPS)-1, p (APTMACl-co-AMPS)-2, and p (APTMACl-co-AMPS)-3 hydrogels.

step continued with a weight loss of 58, 57, and 50%, respectively, in the range of 300–330°C. The final decomposition step ended with a total Weight loss of 98, 98, and 90%, respectively, between 330 and 700°C. So, the amphoteric hydrogels' thermal stability is in between the cationic and anionic hydrogels.

3.2 Swelling Properties of Hydrogels

The swelling properties for bare hydrogels and copolymeric hydrogels are strongly related to the monomer nature, crosslinker ratio, and medium pH (Holback et al., 2011). To evaluate the effect of monomer types and monomer mole ratio on the swelling properties and pH response of hydrogels, dry samples were left to swell until they reach the equilibrium values at room temperature in DI water and in different pH buffer solutions from pH 3.0 to 9.0. In **Figure 3A**, the swelling ratio of p (APTMACl), p (AMPS), p (APTMACl-co-AMPS)-1, p (APTMACl-co-AMPS)-2, and p (APTMACl-co-AMPS)-3 hydrogels in DI water were given as a function of time. All copolymeric hydrogels containing anionic and cationic groups reached equilibrium swelling value almost at about the same time.

As can be seen from **Figure 3A**, all hydrogels swell rapidly in DI water for up to about 1 h and reach a plateau after 8 h. Swelling ratios of hydrogels reaching equilibrium swelling values are in the following order: p (APTMACl) > p (APTMACl-co-AMPS)-1 > p (APTMACl-co-AMPS)-3 > p (AMPS) > p (APTMACl-co-AMPS)-2. The equilibrium swelling values for p (APTMACl), p (APTMACl-co-AMPS)-1, p (APTMACl-co-AMPS)-3, p (AMPS), and p (APTMACl-co-AMPS)-2 hydrogels were calculated as 5,375 ± 752%, 4,390 ± 5%, 3,311 ± 186%, 3,139 ± 882% and 524 ± 120%, respectively. As p (APTMACl) hydrogel has already fixed positive charge in comparison to the anionic hydrogels, p (AMPS) which develops negative charge in DI water *via* dissociation of sulfonic acid groups, the equilibrium swelling ratio of p (APTMACl) is much more than p (AMPS) and the copolymer hydrogels have the swelling values between these two depending on the ratio with exception of p (APTMACl-co-AMPS)-2 as it has an equal amount of anionic and cationic structures, this hydrogel swells to a lesser extent than the others, due to their neutralization of the functional groups.

FIGURE 3 | (A) The swelling Ratio (SR%) of p (APTMACl), p (AMPS), p (APTMACl-co-AMPS)-1, p (APTMACl-co-AMPS)-2, and p (APTMACl-co-AMPS)-3 hydrogels with time, and **(B)** the equilibrium swelling % of p (APTMACl-co-AMPS)-1, p (APTMACl-co-AMPS)-2, and p (APTMACl-co-AMPS)-3 hydrogels at equilibrium time from pH 3.0 to 9.0.
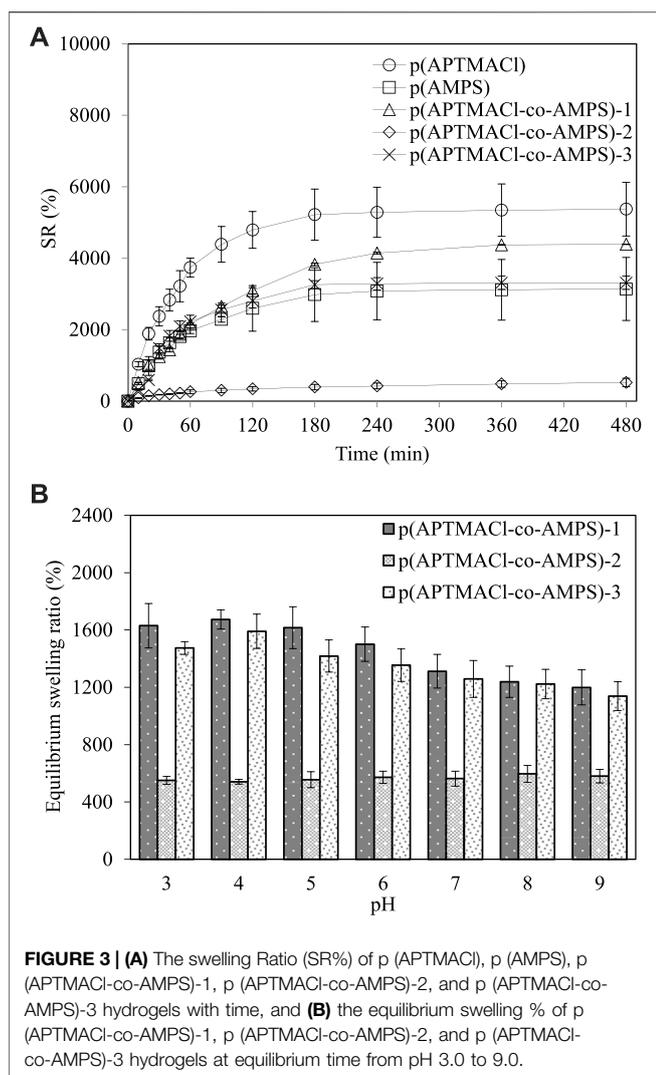
As the used monomers are cationic and anionic character for the preparation of amphoteric hydrogels for (APTMACl-co-AMPS)-1, p (APTMACl-co-AMPS)-2, and p (APTMACl-co-AMPS)-3, the effect of pH on SR% of amphoteric hydrogels were investigated and the corresponding graph was given in **Figure 3B**. The p (APTMACl-co-AMPS)-1 hydrogel exhibits a typical cationic hydrogel swelling behavior where the equilibrium swelling value is high at low pHs and decreases at high pHs. Increasing the pH from 3.0 to 9.0 decreases the equilibrium swelling value from 1,630 ± 155% to 1,200 ± 122%. Interestingly, p (APTMACl-co-AMPS)-3 hydrogel also exhibits a cationic swelling behavior and swells higher at acidic pHs and swell relatively low at basic pHs. The increased pH from 3.0 to 9.0 changes the equilibrium swelling values from 1,475 ± 44% to 1,139 ± 100%. This can be explained in the basic hydrogels swell more at low pHs (under acidic conditions) and decrease swelling due to neutralization of functional groups at high pHs (under basic conditions) (Holback et al., 2011). Since p (APTMACl-co-AMPS)-2 hydrogels contain equal mole ratios of the monomers, the equilibrium swelling values are almost stable at all pH

conditions such as acidic, neutral, and basic. In conclusion, the p (APTMACl-co-AMPS)-1 and p (APTMACl-co-AMPS)-3 hydrogels are versatile and possesses higher ionization capability and affords greater swelling capability under acidic pH conditions. On the contrary, these hydrogels also reveal lesser swelling ability under basic pH conditions.

3.3 Dye Removal From Aqueous Medium *via* Hydrogels

3.3.1 Effect of Ionic Nature of Adsorbents on Adsorption of Dyes (MB, MO and EY)

The dye adsorption from the aqueous medium with prepared anionic, cationic, and amphoteric hydrogels was carried out at room temperature. Firstly, the prepared hydrogels were placed into 50 ml of 100 ppm aqueous MB, MO, and EY solutions, separately. The adsorbed amounts of dyes from aqueous media with prepared hydrogels were given in **Figure 4A**. It was observed that there is no adsorption were observed for cationic dye (MB) by p (APTMACl) hydrogels, and anionic dyes (MO and EY) by anionic hydrogels. On the other hand, cationic p (APTMACl) hydrogels adsorbed 47.6 ± 1.3 mg/g of MO, and 42.5 ± 1.9 mg/g of EY, whereas the adsorbed amount of MB was calculated as 48.8 ± 1.1 mg/g with anionic p (AMPS) hydrogels from 50 ml 50 ppm aqueous solution of related components.

Moreover, the prepared amphoteric hydrogels from the various mole ratio of cationic APTMACl and anionic AMPS monomers were also used in the removal of dyes from aqueous solutions. The p (APTMACl-co-AMPS)-1 hydrogels behaved as cationic gels as expected due to 3 fold higher content of cationic APTMACl monomer. Therefore, 45.6 ± 1.1 mg/g of MO and 49.4 ± 0.2 mg/g of EY were removed by p (APTMACl-co-AMPS)-1 hydrogels, whereas there is no adsorption was observed for MB dyes from aqueous solutions of related dyes at concentration of 50 ppm in 50 ml. Similarly, the prepared p (APTMACl-co-AMPS)-2 hydrogels showed cationic behavior as well contrary to what was expected and didn't adsorb cationic MB dye, however, 16.7 ± 2.6 mg/g of MO and 18.2 ± 1.7 mg/g of EY from their 50 ml 50 ppm aqueous solutions were adsorbed by this hydrogel. Since p (APTMACl-co-AMPS)-3 hydrogels contained 3-fold more anionic AMPS monomer in their structure, MB dye was adsorbed the most amount, 48.1 ± 0.7 mg/g. However, 1.7 ± 02 and 2.7 ± 0.2 mg/g MO and EY dyes were also adsorbed by p (APTMACl-co-AMPS)-3 hydrogels from their 50 ml 50 ppm aqueous solutions, respectively. Unlike the other copolymeric hydrogels prepared in this study, p (APTMACl-co-AMPS)-3 hydrogels showed slightly amphoteric properties due to the difference in the positive and negative charges strength of the corresponding moieties in the copolymeric network.

3.3.2 The Effect of Acid/Based Treatment of Amphoteric Hydrogels on Adsorption of Dyes

As the higher amounts of EY and MO was removed by the prepared amphoteric hydrogels, MB and EY dyes were chosen to investigate the effect of HCl/NaOH treatments of the hydrogels on adsorption ability, and the corresponding graph is given in **Figures 4B,C,D**, respectively. In the

FIGURE 4 | (A) The adsorbed amounts of MB, MO, and EY dyes by cationic p (APTMACl), anionic p (AMPS) and amphoteric p (APTMACl-co-AMPS) hydrogels, and the change on dye adsorption capacities of amphoteric (B) p (APTMACl-co-AMPS)-1, (C) p (APTMACl-co-AMPS)-2, and (D) p (APTMACl-co-AMPS)-3 hydrogels after HCl and NaOH treatment. (Adsorption conditions: 50 mg hydrogel, 50 ml 50 ppm MB and EY solutions, 500 rpm stirring rate, room temperature).

adsorption studies performed after the HCl and NaOH treatments of copolymeric hydrogels separately, it was observed that the treatment of hydrogels with HCl or NaOH strongly affected the amount of adsorbed dye from their aqueous solutions. In **Figure 4B**, even the untreated form of p (APTMACl-co-AMPS)-1 hydrogels acting as cationic hydrogels (no adsorption for MB), and the HCl and NaOH treated p (APTMACl-co-AMPS)-1 hydrogels adsorbed 1.1 ± 0.2, and 4.3 ± 1.8 mg/g of MB while absorbing 46.5 ± 0.1, and 38.6 ± 1.6 mg/g of EY from 50 ml 50 ppm aqueous solution of the dye.

On the other hand, in **Figure 4C**, the HCl and NaOH treated p (APTMACl-co-AMPS)-2 hydrogels also didn't adsorb any MB dye, and the untreated p (APTMACl-co-AMPS)-2 hydrogels, however, adsorbed some EY, 18.2 ± 1.7 mg/g and the adsorption amount of this dye is increased after HCl and NaOH treatment to 37.2 ± 1.6 mg/g, and 28.8 ± 1.5 mg/g, respectively. Moreover, as illustrated in **Figure 4D**, the treatment of p (APTMACl-co-AMPS)-3 hydrogels with HCl afforded 47.5 ± 0.9 mg/g MB, and 10.7 ± 0.1 mg/g EY adsorption from their 50 ml 50 ppm aqueous solutions, whereas NaOH treated p (APTMACl-co-AMPS)-3 hydrogels adsorbed 46.3 ± 1.8 mg/g of MB, and

FIGURE 5 | (A) The effect of pH on adsorption of MB and EY by HCl-treated p (APTMACl-co-AMPS)-3 hydrogels, and (B) the adsorbed amount of MB and EY by HCl-treated p (APTMACl-co-AMPS)-3 hydrogels with time. (Adsorption conditions: 50 mg hydrogel, 50 ml 50 ppm MB and EY solutions, 500 rpm stirring rate, room temperature).
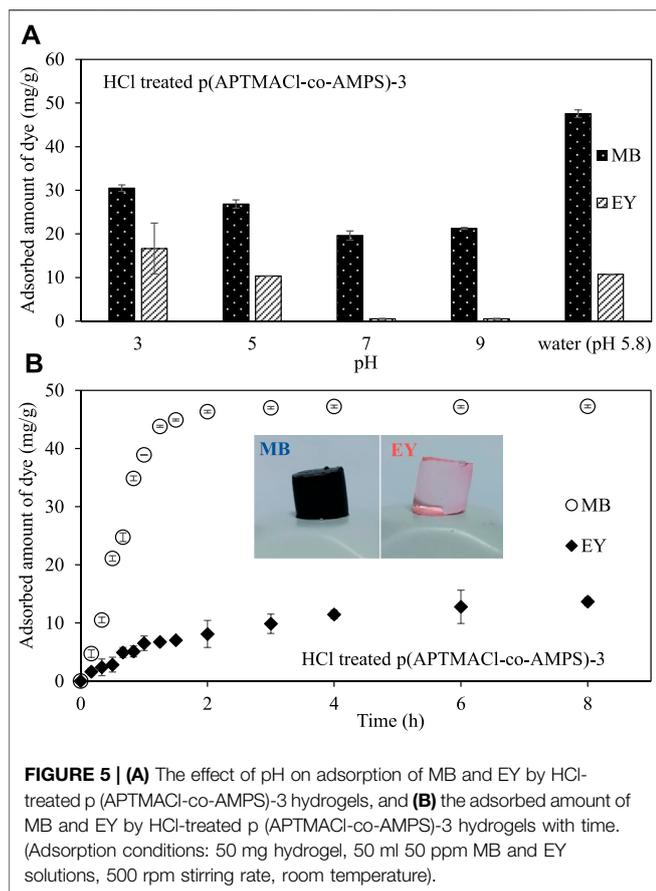
3.1 ± 1.8 mg/g of EY, respectively. To summarize, the HCl and NaOH treatment of the copolymeric p (APTMACl-co-AMPS) hydrogels are very effective in their cationic (MB) or anionic (EY) removal ability from aqueous solutions. Therefore, amphoteric p (APTMACl-co-AMPS) hydrogels are versatile and can be tuned in terms of composition and can be tuned or activated effectively by acid and base treatment removal of charged dyes from aquatic environments. The observed higher dye adsorption capability of p (APTMAC-co-AMPS)-3 hydrogels after HCl treatment can be explain with the elimination of possible electrostatic interactions between -$^+$N(CH$_3$)$_3$ and -SO$_3^-$ functional groups of AMPS and APTMACl in the hydrogel structure (Gad, 2008; Mahida and Patel, 2016; Wei et al., 2016). Therefore, the increase in the number of functional groups that can interact with the dye molecules in comparison to the interaction of these functional groups with each other can cause an increase in the amount of adsorbed dye.

3.3.3 Effect of pH on Dye Adsorption
As the pH is one of the most important parameters for the adsorption studies, the effect of pH on adsorption of MB and EY from the 50 ml 50 ppm solution in 500 mM sodium phosphate buffer at various pH values, 3.0, 5.0, 7.0, and 9.0 by HCl-treated p (APTMACl-co-AMPS)-3 hydrogels were investigated. As shown in **Figure 5A**, the pH of the dye solution directly affected the amount of adsorbed MB and EY by HCl-treated p (APTMACl-

co-AMPS)-3 hydrogels. The amount of adsorbed MB was calculated as 30.5 ± 0.7, 26.8 ± 0.9, 19.6 ± 1.1, and 21.2 ± 0.9 mg/g from the 50 ml 50 ppm solutions in 500 mM sodium phosphate buffer at pH 3.0, 5.0, 7.0, and 9.0, respectively. On the other hand, a similar adsorption profile was observed for EY at various pH values and from 50 ml 50 ppm solution of EY in 500 mM sodium phosphate buffer at pH 3.0 and 5.0, 16.6 ± 5.8, and 10.3 ± 0.4 mg/g EY adsorption were done by HCl-treated p (APTMACl-co-AMPS)-3 hydrogels, respectively. On the other hand, there is no adsorption was observed at pH 7 and 9, respectively.

Moreover, the time-dependent adsorption of MB and EY by HCl-treated p (APTMACl-co-AMPS)-3 hydrogels from their 50 ml 50 ppm aqueous solution and the corresponding graph was shown in **Figure 5B**. It was observed that the adsorption of both MB and EY dyes by HCl-treated p (APTMACl-co-AMPS)-3 hydrogels were almost completed in 2 h with the calculated adsorbed amounts were 46.3 ± 0.2, and 8.1 ± 2.3 mg/g, respectively. However, the adsorption of MB and EY dyes by HCl-treated p (APTMACl-co-AMPS)-3 hydrogels slightly continued up to 8 h, and a cumulative of 47.3 ± 0.2, and 13.7 ± 0.7 mg/g MB and EY adsorption was achieved, respectively.

3.3.4 Effect of Dye Concentration on the Adsorption Capacity
To investigate the effect of dye concentration on the adsorption capacity of HCl-treated p (APTMACl-co-AMPS)-3 hydrogels, the amount of hydrogel was kept constant as 0.05 mg, and the amount of dye adsorbed after 6 h was calculated from 50 ml of 10, 25, 50, 75 and 100 ppm dye solutions. As illustrated in **Figure 6A**, the adsorbed amount of MB from 50 ml aqueous solution at various concentrations shows a linear increase profile with the increase in the concentration of dye solutions.

The HCl-treated p (APTMACl-co-AMPS)-3 hydrogels adsorbed 9.6 ± 0.1, 24.2 ± 0.1, 47.5 ± 0.9, 73.4 ± 0.3, and 98.8 ± 0.1 mg/g of MB from 50 ml of aqueous solutions at 10, 25, 50, 75, and 100 ppm concentrations, respectively. Similarly, the amount of adsorbed EY from its 50 ml aqueous solutions at various concentrations was given in **Figure 6B**. Accordingly, a somewhat similar trend was observed and the adsorbed amount of EY by HCl-treated p (APTMACl-co-AMPS)-3 hydrogels was found to increase from 6.6 ± 0.1 mg/g to 8.5 ± 0.2, 10.7 ± 0.1, 17.4 ± 1.1, and 18.3 ± 1.8 mg/g for 50 ml of 10, 25, 50, 75, and 100 ppm EY concentrations, respectively.

3.4 Adsorption Kinetics
The kinetic parameters for MB and EY adsorption by HCl-treated p (APTMACl-co-AMPS)-3 hydrogels were calculated to describe the rate and mechanism of adsorption. For this purpose, two of the most widely used kinetic models, e.g., the pseudo-first-order and pseudo-second-order kinetic models were applied to MB and EY dye adsorption by HCl-treated p (APTMACl-co-AMPS)-3 hydrogels. The graphs for pseudo-first-order and pseudo-second-order kinetic models of 1.5 h of adsorption time for MB and EY by HCl-treated p (APTMACl-co-AMPS)-3 hydrogels were applied and the corresponding graphs were given in **Supplementary Figure S1**.

FIGURE 6 | The effect of dye concentration on the adsorption of **(A)** MB, and **(B)** EY by HCl-treated p (APTMACl-co-AMPS)-3 hydrogels. (Adsorption conditions: 50 mg hydrogel, 50 ml MB and EY solutions, 500 rpm stirring rate, room temperature).
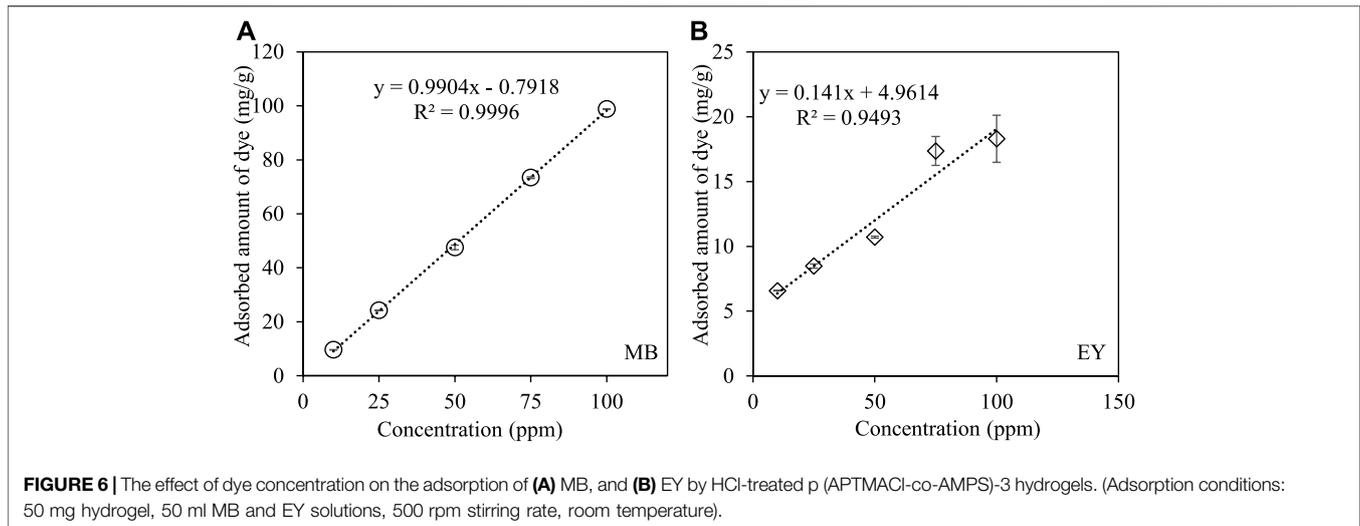
TABLE 1 | The pseudo-first and pseudo-second-order kinetic constants and their respective correlation coefficients for the adsorption of MB and EY by HCl-treated p (APTMACl-co-AMPS)-3 hydrogels.

Dye	Exp.	Pseudo-first-order kinetics			Pseudo-second-order kinetics		
	q_e (mg.g^{-1})	q_e (mg.g^{-1})	k_1	R^2	q_e (mg.g^{-1})	k_2	R^2
MB	47.5 ± 1.2	80.1	2.3	0.97	1,250	2.2E-5	0.01
EY	10.7 ± 0.1	12.9	0.5	0.93	15.9	0.03	0.70

TABLE 2 | The adsorption parameters of MB and EY by HCl-treated p (APTMACl-co-AMPS)-3 hydrogels from the Langmuir, Freundlich, Temkin, and Dubinin-Radushkevich isotherms.

Dye	Exp.	Langmuir			Freundlich		
	q_e (mg.g^{-1})	K_L (ml.mg^{-1})	q_m (mg.g^{-1})	R^2	K_F (mg.g^{-1})	n	R^2
MB	47.5 ± 1.2	2.73	51.5	0.96	34.5	0.76	0.98
		Temkin			**Dubinin-Radushkevich**		
		K_T	b	R^2	q_m	β	R^2
		139.8	265.1	0.93	92.5	2E-7	0.93

Dye	Exp.	Langmuir			Freundlich		
	q_e (mg.g^{-1})	K_L (ml.mg^{-1})	q_m (mg.g^{-1})	R^2	K_F (mg.g^{-1})	n	R^2
EY	10.7 ± 0.1	0.008	20.9	0.96	4.0	3.14	0.88
		Temkin			**Dubinin-Radushkevich**		
		K_T	b	R^2	q_m	β	R^2
		34.1	713.9	0.79	13.1	2E-6	0.52

The values of the kinetic variables of q_e, k_1, and k_2 which are crucial in understanding the adsorption kinetics of MB and EY dyes were calculated from the related graphs in **Supplementary Figure S1** and summarized in **Table 1**.

From the calculated values, the adsorption of both MB and EY dyes from the aqueous medium by HCl-treated p (APTMACl-co-AMPS)-3 hydrogels revealed a better fit to pseudo-first-order with higher correlation coefficient values as 0.97, and 0.93, respectively. The q_e values for MB and EY adsorption of HCl-treated p (APTMACl-co-AMPS)-3 hydrogels were calculated as

80.1, and 12.9 mg/g, whereas the q_e values for MB and EY adsorption by HCl-treated p (APTMACl-co-AMPS)-3 hydrogels were determined as 47.5 ± 1.2, and 10.7 ± 0.1 mg/g, respectively. As a result, the rate of change of solute uptake with time in MB and EY adsorption studies by HCl-treated p (APTMACl-co-AMPS)-3 hydrogels is assumed to be directly proportional to the difference in saturation concentration and the amount of solid removal with time, which is generally applicable over the initial stage of an adsorption process (Sahoo and Prelot, 2020).

FIGURE 7 | (A) The UV-Vis spectra of simultaneous MB and EY adsorption from 50 ppm MB-EY mixture solution by HCl-treated p (APTMACl-co-AMPS)-3 hydrogels, and **(B)** the effect of dye mixture concentration on simultaneous adsorption of MB-EY from the mixture solution. (Adsorption conditions: 50 mg hydrogel, 50 ml MB-EY mixture solutions, 500 rpm stirring rate, room temperature).
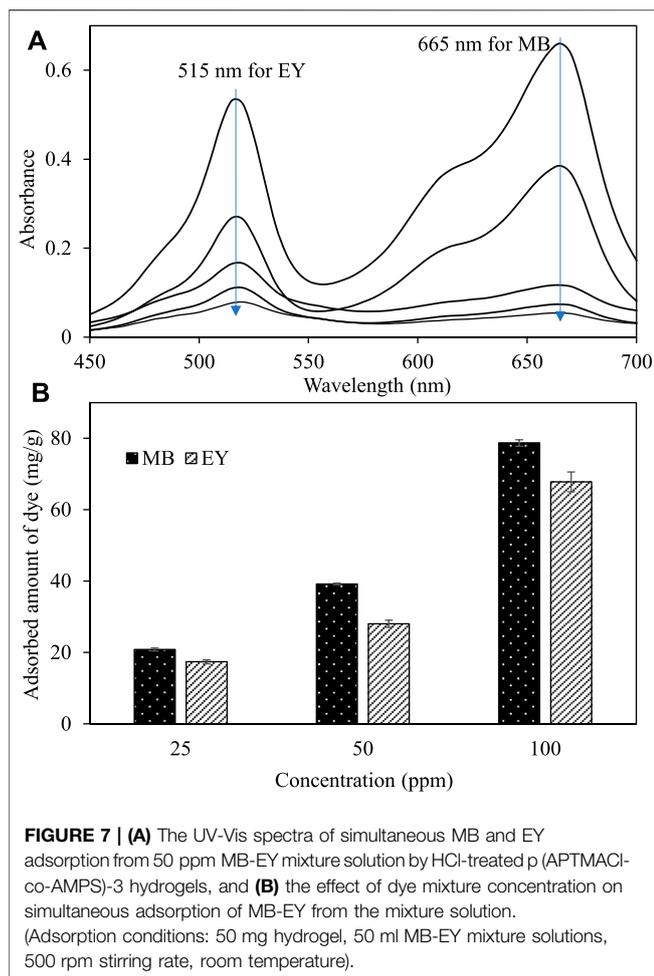
3.5 Adsorption Isotherms

The four well-known adsorption isotherms are Langmuir, Freundlich, Temkin, and Dubinin-Radushkevich isotherms and were applied to the adsorption of MB and EY dyes by HCl-treated p (APTMACl-co-AMPS)-3 hydrogels by using the data from **Figures 6A,B**, respectively. The corresponding graphs of isotherms for MB and EY adsorption by HCl-treated p (APTMACl-co-AMPS)-3 hydrogels were given in **Supplementary Figure S2**, and **Supplementary Figure S3**, respectively. The calculated isotherm constants and correlation coefficients from **Supplementary Figure S2**, and **Supplementary Figure S3** were summarized in **Table 2**.

It was determined that the adsorption of MB by HCl-treated p (APTMACl-co-AMPS)-3 hydrogels compatible with Freundlich isotherm with 0.98 correlation coefficient value, whereas Langmuir isotherm was found as the best fit for the absorption of EY by HCl-treated p (APTMACl-co-AMPS)-3 hydrogels with 0.96 correlation coefficient value. According to the Freundlich isotherm, it is assumed that as the adsorbent concentration increases, the adsorbent concentration on the adsorbent surface also increases (Hamdaoui and Naffrechoux, 2007). The K_F constant was calculated as 34.5 mg/g and the n constant was determined as 0.75 for MB adsorption. The

Langmuir isotherm constants such as K_L and q_m were calculated as 0.008 ml/mg, and 20.1 mg/g, respectively for the EY adsorption by HCl-treated p (APTMACl-co-AMPS)-3 hydrogels.

3.6 Simultaneous Removal of Dyes From Aqueous Media

In wastewaters, usually, more than one pollutant is present at various types of structures and charges such as anionic, cationic, neutral, and amphoteric, etc. Therefore, the preparation of adsorbents that can remove more than one pollutant from wastewaters is of noticeable importance. The adsorption ability of the HCl-treated p (APTMACl-co-AMPS) hydrogels for both cationic (MB) and anionic (EY) dyes from their individual aqueous solutions were shown. Therefore, the possible adsorption of MB-EY from their mixture solution in water at various concentrations was also investigated, and the corresponding graph is given in **Figure 7**. The UV-Vis spectra of adsorption study of both MB and EY dyes from their 50 ml 50 ppm MB and EY mixture solution by HCl-treated p (APTMACl-co-AMPS) hydrogels were shown in **Figure 7A**. It was clearly seen that the adsorption peaks of MB and EY at 665 and 515 nm were decreased with time.

On the other hand, the adsorbed amounts of both MB and EY dyes from their 50 ml 25, 50, and 100 ppm MB/EY mixture solution by HCl-treated p (APTMACl-co-AMPS) hydrogels were given in **Figure 7B**. It is apparent that with the increase in the concentration of dye mixture solutions, the adsorbed MB and EY amounts were also increased. The calculated amount of adsorbed MB from 50 ml 25, 50, and 100 ppm MB/EY mixture solutions were calculated as 20.8 ± 0.4, 39.2 ± 0.2, and 78.7 ± 0.9 mg/g, whereas the adsorbed amount of EY was calculated as 17.4 ± 0.6, 28.1 ± 1.1, and 67.8 ± 2.8 mg/g, respectively. The trend of the higher amount of dye adsorption with the increase of the dye concentration from dye mixture is similar to that of their individual adsorption suggesting the higher amounts of dye absorption capabilities of the HCl-treated p (APTMACl-co-AMPS) hydrogels.

The comparison of the obtained results in terms of q_e (mg/g), adsorption kinetics, and the adsorption types with the similar studies reported in the literature was given in **Table 3**. In this study, the maximum adsorption capacity of HCl-treated p (APTMACl-co-AMPS)-3 hydrogels for MB and EY was calculated as 78.7 ± 0.9 and 67.8 ± 2.8 mg/g from their corresponding 50 ml 100 ppm mixture solutions, respectively. The adsorption behavior of HCl-treated p (APTMACl-co-AMPS)-3 hydrogels for both MB and EY fitted with pseudo second order (PSO) kinetic model. Moreover, the MB adsorption by HCl-treated p (APTMACl-co-AMPS)-3 hydrogels fitted with Freundlich model, whereas the EY adsorption by HCl-treated p (APTMACl-co-AMPS)-3 hydrogels fitted with Langmuir model.

It was reported that carboxymethyl cellulose sodium/graphene oxide hydrogels were adsorbed 58.2 mg/g of MB and 65.7 mg/g of EY from their corresponding aqueous solution (Liu et al., 2016). On the other hand, carbon nanotube incorporated eucalyptus derived activated carbons adsorbed 43.4 mg/g of MB and

TABLE 3 | Comparison of q_e (mg/g), adsorption kinetics, and adsorption type of HCl-treated p (APTMACl-co-AMPS)-3 hydrogels with reported other materials.

Materials	Dye	Qe (mg/g)	Kinetic model	İsotherm model	REF
HCl-treated p(APTMACl-co-AMPS)-3	MB	78.7	PFO	Freundlich	This study
	EY	67.8		Langmuir	
Carboxymethyl cellulose sodium/graphene oxide hydrogel	MB	58.2	PSO	Langmuir	Liu et al. (2016)
	EY	65.7			
Carbon nanotube incorporated eucalyptus derived activated carbon	MB	43,4	PSO	Dubinin-Radushkevich	Yadav et al. (2022)
	EY	49,0			
Chitosan/polyacrylate/graphene oxide composite physical hydrogel	MB	296.5	PFO	—	Chang et al. (2020)
	FY3*	280.3	PSO		
Chitosan beads	MY**	1.33	Both PFO and PSO	Langmuir	Chiou and Chuang, (2006)
	RB15**	0.72			
Banana pseudo-stem derived superabsorbent hydrogels	MB	333.4	PSO	Freundlich	Bello et al. (2018)
	MO	124.0			
Chitosan-starch (ChS) hydrogel	DR80***	312.8	PSO	Freundlich	Ngwabebhoh et al. (2016)
Poly(methacrylic acid)/zeolite hydrogel composites	BY28****	33.7	PFO	Langmuir	Panic and Velickovic, (2014)
N-containing biopolymer-based nanochitin hydrogel	MB	531	Both PFO and PSO	Both Langmuir and Freundlich	Zhang et al. (2019)
	As(III)	217	PSO		

*Food yellow 3, ** Direct red 80, *** Basic yellow 28; a Pseudo first order, b Pseudo second order.

TABLE 4 | Distribution (K_d) and selectivity (k) coefficients of HCl-treated p (APTMACl-co-AMPS)-3 hydrogels for the adsorption of MB and EY from their mix solutions at different concentration.

Parameter	K_d (L.g^{-1})		
Dyes	**25 ppm MB/EY**	**50 ppm MB/EY**	**100 ppm MB/EY**
MB	5.1 ± 0.64	3.7 ± 0.08	3.9 ± 0.23
EY	2.3 ± 0.25	1.3 ± 0.11	2.3 ± 0.29
Parameter	k		
Dyes	**25 ppm MB/EY**	**50 ppm MB/EY**	**100 ppm MB/EY**
MB	2.1 ± 0.04	2.8 ± 0.16	1.7 ± 0.12
EY	0.5 ± 0.08	0.3 ± 0.02	0.6 ± 0.04

49.0 mg/g of EY, respectively (Yadav et al., 2022). Bello et al. (2018), reported that the prepared banana pseudo-stem derived superabsorbent hydrogels adsorbed both cationic MB and anionic MO dyes with 333.4 and 124.0 mg/g, respectively. Moreover, the effective removal of both dye (MB) and heavy metal ion [As(III)] from aqueous solution with N-containing biopolymer-based nanochitin hydrogels was also reported in literature (Zhang et al., 2019). Therefore, it is apparent that the obtained results in this study are comparable with similar studies reported as adsorbents for the relevant dyes and can be used for multiple dye removal due to the amphoteric nature.

3.7 Adsorption Coefficients

Form the simultaneous MB and EY adsorption for HCl-treated p (APTMACl-co-AMPS)-3 hydrogels the important adsorption coefficients such as distribution (K_d) and selectivity (k) can be calculated. For this purpose, 50 mg of HCl-treated p (APTMACl-co-AMPS)-3 hydrogels were used for the adsorption from 50 ml of 25, 50, and 100 ppm MB-EY dye mixtures, and corresponding coefficients are summarized in **Table 4**. The K_d values of HCl-treated p (APTMACl-co-AMPS)-3 hydrogels for MB in 25, 50, and 100 ppm mixtures of MB-EY were calculated as 5.1 ± 0.6, 3.7 ± 0.1, and 3.9 ± 0.2 g/L, respectively, whereas the K_d values for EY adsorption in 25, 50, and 100 ppm mixtures of MB-EY were calculated as 2.3 ± 0.2, 1.3 ± 0.1, and 2.3 ± 0.3 g/L, respectively. The higher K_d values for MB suggest the higher binding tendency of MB than EY on HCl-treated p (APTMACl-co-AMPS)-3 hydrogels.

On the other hand, the calculated *k* values of HCl-treated p (APTMACl-co-AMPS)-3 hydrogels showed that the selectivity of the hydrogels for MB was 5-fold higher than EY in 25 ppm mixture of MB-EY. Similarly, the HCl-treated p (APTMACl-co-AMPS)-3 hydrogels were at least 9-fold more selective for MB than EY with k values of 2.8 ± 0.1, and 0.3 ± 0.1, respectively, from 50 ppm MB-EY mixture. On the other hand, the selectivity of HCl-treated p (APTMACl-co-AMPS)-3 hydrogels to MB was determined as 3-fold higher than EY in 100 ppm of MB/EY mixture. The increase of dye concentrations causes a relative decrease in the selectivity of HCl-treated p (APTMACl-co-AMPS)-3 hydrogels due to the higher solution concentration of the dyes as their diffusion onto the hydrogels were also increased.

4 CONCLUSION

In this study, simultaneous free radical polymerization and crosslinking of cationic p (APTMACl), anionic p (AMPS), and amphoteric p (APTMACl-co-AMPS) hydrogels were reported. Because of the charged nature of the prepared hydrogels, the prepared cationic hydrogels adsorbed anionic MO and EY dye whereas the anionic p (AMPS) hydrogels adsorbed cationic MB dyes as anticipated. Moreover, the copolymeric p (APTMACl-co-AMPS)-1 and p (APTMACl-co-AMPS)-2 hydrogels were prepared at various mole ratios of the cationic and anionic moieties to attain amphoteric hydrogels and to demonstrate the

versatility of the hydrogels. Furthermore, HCl and NaOH treatment of amphoteric p (APTMACl-co-AMPS)-3 hydrogels further activate increase the dye adsorption capability of the prepared amphoteric hydrogels for both MB and EY dyes from their aqueous solutions, and the amount of adsorbed MB and EY increased with the HCl and NaOH treatment of the hydrogels. Moreover, prepared HCl-treated p (APTMACl-co-AMPS)-3 hydrogels exhibited multiple dye removal capabilities from their aqueous mixture of the dye solutions.

DATA AVAILABILITY STATEMENT

The original contributions presented in the study are included in the article/**Supplementary Material**, further inquiries can be directed to the corresponding author.

REFERENCES

Abdi, J., Vossoughi, M., Mahmoodi, N. M., Alemzadeh, I., and Vossoughi, M. (2017). Synthesis of Metal-Organic Framework Hybrid Nanocomposites Based on GO and CNT with High Adsorption Capacity for Dye Removal. *Chem. Eng. J.* 326, 1145–1158. doi:10.1016/j.cej.2017.06.054

A. K. Rathoure and V. K. Dhatwalia (Editors) (2016). *Toxicity and Waste Management Using Bioremediation* (IGI Global). doi:10.4018/978-1-4666-9734-8

Anjaneyulu, Y., Sreedhara Chary, N., and Samuel Suman Raj, D. (2005). Decolourization of Industrial Effluents - Available Methods and Emerging Technologies - A Review. *Rev. Environ. Sci. Biotechnol.* 4, 245–273. doi:10.1007/s11157-005-1246-z

Bello, K., Sarojini, B. K., Narayana, B., Rao, A., and Byrappa, K. (2018). A Study on Adsorption Behavior of Newly Synthesized Banana Pseudo-stem Derived Superabsorbent Hydrogels for Cationic and Anionic Dye Removal from Effluents. *Carbohydr. Polym.* 181, 605–615. doi:10.1016/j.carbpol.2017.11.106

Cao, M., Shen, Y., Yan, Z., Wei, Q., Jiao, T., Shen, Y., et al. (2021). Extraction-like Removal of Organic Dyes from Polluted Water by the Graphene Oxide/PNIPAM Composite System. *Chem. Eng. J.* 405, 126647. doi:10.1016/j.cej.2020.126647

Cao, M., Zhuang, Z., Liu, Y., Zhang, Z., Xuan, J., Zhang, Q., et al. (2022). Peptide-mediated green Synthesis of the MnO2@ZIF-8 Core-Shell Nanoparticles for Efficient Removal of Pollutant Dyes from Wastewater via a Synergistic Process. *J. Colloid Interf. Sci.* 608, 2779–2790. doi:10.1016/j.jcis.2021.11.003

Chang, Z., Chen, Y., Tang, S., Yang, J., Chen, Y., Chen, S., et al. (2020). Construction of Chitosan/polyacrylate/graphene Oxide Composite Physical Hydrogel by Semi-dissolution/acidification/sol-gel Transition Method and its Simultaneous Cationic and Anionic Dye Adsorption Properties. *Carbohydr. Polym.* 229, 115431. doi:10.1016/j.carbpol.2019.115431

Chiou, M.-S., and Chuang, G.-S. (2006). Competitive Adsorption of Dye Metanil Yellow and RB15 in Acid Solutions on Chemically Cross-Linked Chitosan Beads. *Chemosphere* 62, 731–740. doi:10.1016/j.chemosphere.2005.04.068

Crini, G., and Lichtfouse, E. (2019). Advantages and Disadvantages of Techniques Used for Wastewater Treatment. *Environ. Chem. Lett.* 17, 145–155. doi:10.1007/s10311-018-0785-9

Dargahi, M., Ghasemzadeh, H., and Bakhtiary, A. (2018). Highly Efficient Absorption of Cationic Dyes by Nano Composite Hydrogels Based on κ-carrageenan and Nano Silver Chloride. *Carbohydr. Polym.* 181, 587–595. doi:10.1016/j.carbpol.2017.11.108

Das, S., Chakraborty, P., Ghosh, R., Paul, S., Mondal, S., Panja, A., et al. (2017). Folic Acid-Polyaniline Hybrid Hydrogel for Adsorption/Reduction of Chromium(VI) and Selective Adsorption of Anionic Dye from Water. *ACS Sustain. Chem. Eng.* 5, 9325–9337. doi:10.1021/acssuschemeng.7b02342

Das, S., Chakraborty, P., Shit, A., Mondal, S., and Nandi, A. K. (2016). Robust Hybrid Hydrogels with Good Rectification Properties and Their Application as

AUTHOR CONTRIBUTIONS

Formal analysis, SD and BA. Investigation, SD, BA, NA, and NS. Methodology, SD and BA. Writing—original draft preparation, SD and BA. Conceptualization, NA and NS. Project administration, NS. Resources, NS. Supervision, NA and NS. Writing—review and editing, NA and NS. Funding acquisition, NS. Visualization, NA and NS. All authors have read and agreed to the published version of the manuscript.

SUPPLEMENTARY MATERIAL

The Supplementary Material for this article can be found online at: https://www.frontiersin.org/articles/10.3389/fmats.2022.837701/full#supplementary-material

Active Materials for Dye-Sensitized Solar Cells: Insights from AC Impedance Spectroscopy. *J. Mater. Chem. A.* 4, 4194–4210. doi:10.1039/C5TA08833J

De Gisi, S., Lofrano, G., Grassi, M., and Notarnicola, M. (2016). Characteristics and Adsorption Capacities of Low-Cost Sorbents for Wastewater Treatment: A Review. *Sustain. Mater. Tech.* 9, 10–40. doi:10.1016/j.susmat.2016.06.002

El-Hamshary, H., El-Sigeny, S., Abou Taleb, M. F., and El-Kelesh, N. A. (2007). Removal of Phenolic Compounds Using (2-hydroxyethyl Methacrylate/acrylamidopyridine) Hydrogel Prepared by Gamma Radiation. *Sep. Purif. Tech.* 57, 329–337. doi:10.1016/j.seppur.2007.04.013

Gad, Y. H. (2008). Preparation and Characterization of Poly(2-Acrylamido-2-Methylpropane-Sulfonic acid)/Chitosan Hydrogel Using Gamma Irradiation and its Application in Wastewater Treatment. *Radiat. Phys. Chem.* 77, 1101–1107. doi:10.1016/j.radphyschem.2008.05.002

Gan, L., Li, H., Chen, L., Xu, L., Liu, J., Geng, A., et al. (2018). Graphene Oxide Incorporated Alginate Hydrogel Beads for the Removal of Various Organic Dyes and Bisphenol A in Water. *Colloid Polym. Sci.* 296, 607–615. doi:10.1007/s00396-018-4281-3

Gupta, V. K., and Suhas (2009). Application of Low-Cost Adsorbents for Dye Removal - A Review. *J. Environ. Manage.* 90, 2313–2342. doi:10.1016/j.jenvman.2008.11.017

Hai, F. I., Yamamoto, K., and Fukushi, K. (2007). Hybrid Treatment Systems for Dye Wastewater. *Crit. Rev. Environ. Sci. Tech.* 37, 315–377. doi:10.1080/10643380601174723

Hamdaoui, O., and Naffrechoux, E. (2007). Modeling of Adsorption Isotherms of Phenol and Chlorophenols onto Granular Activated carbonPart I. Two-Parameter Models and Equations Allowing Determination of Thermodynamic Parameters. *J. Hazard. Mater.* 147, 381–394. doi:10.1016/j.jhazmat.2007.01.021

Holback, H., Yeo, Y., and Park, K. (2011). "Hydrogel Swelling Behavior and its Biomedical Applications," in *Biomedical Hydrogels* (Elsevier), 3–24. doi:10.1533/9780857091383.1.3

Katheresan, V., Kansedo, J., and Lau, S. Y. (2018). Efficiency of Various Recent Wastewater Dye Removal Methods: A Review. *J. Environ. Chem. Eng.* 6, 4676–4697. doi:10.1016/j.jece.2018.06.060

Kubilay, S., Demirci, S., Can, M., Aktas, N., and Sahiner, N. (2021). Dichromate and Arsenate Anion Removal by PEI Microgel, Cryogel, and Bulkgel. *J. Environ. Chem. Eng.* 9, 104799. doi:10.1016/j.jece.2020.104799

Leverenz, H. L., and Asano, T. (2011). "Wastewater Reclamation and Reuse System," in *Treatise on Water Science* (Elsevier), 63–71. doi:10.1016/B978-0-444-53199-5.00076-2

Liu, J., Chu, H., Wei, H., Zhu, H., Wang, G., Zhu, J., et al. (2016). Facile Fabrication of Carboxymethyl Cellulose Sodium/graphene Oxide Hydrogel Microparticles for Water Purification. *RSC Adv.* 6, 50061–50069. doi:10.1039/C6RA06438H

Mahida, V. P., and Patel, M. P. (2016). Superabsorbent Amphoteric Nanohydrogels: Synthesis, Characterization and Dyes Adsorption Studies. *Chin. Chem. Lett.* 27, 471–474. doi:10.1016/j.cclet.2015.12.015

Mojsov, K., Andronikov, D., Janevski, A., Kuzelov, A., and Gaber, S. (2016). The Application of Enzymes for the Removal of Dyes from Textile Effluents. *Adv. Techn* 5, 81–86. doi:10.5937/savteh1601081M

Ngwabebhoh, F. A., Gazi, M., and Oladipo, A. A. (2016). Adsorptive Removal of Multi-Azo Dye from Aqueous Phase Using a Semi-IPN Superabsorbent Chitosan-Starch Hydrogel. *Chem. Eng. Res. Des.* 112, 274–288. doi:10.1016/j.cherd.2016.06.023

Okesola, B. O., and Smith, D. K. (2016). Applying Low-Molecular Weight Supramolecular Gelators in an Environmental Setting - Self-Assembled Gels as Smart Materials for Pollutant Removal. *Chem. Soc. Rev.* 45, 4226–4251. doi:10.1039/C6CS00124F

Panic, V. V., and Velickovic, S. J. (2014). Removal of Model Cationic Dye by Adsorption onto Poly(methacrylic Acid)/zeolite Hydrogel Composites: Kinetics, Equilibrium Study and Image Analysis. *Sep. Purif. Tech.* 122, 384–394. doi:10.1016/j.seppur.2013.11.025

Rafatullah, M., Sulaiman, O., Hashim, R., and Ahmad, A. (2010). Adsorption of Methylene Blue on Low-Cost Adsorbents: A Review. *J. Hazard. Mater.* 177, 70–80. doi:10.1016/j.jhazmat.2009.12.047

Sahiner, N., and Seven, F. (2015). A Facile Synthesis Route to Improve the Catalytic Activity of Inherently Cationic and Magnetic Catalyst Systems for Hydrogen Generation from Sodium Borohydride Hydrolysis. *Fuel Process. Tech.* 132, 1–8. doi:10.1016/j.fuproc.2014.12.008

Sahiner, N. (2013). Soft and Flexible Hydrogel Templates of Different Sizes and Various Functionalities for Metal Nanoparticle Preparation and Their Use in Catalysis. *Prog. Polym. Sci.* 38, 1329–1356. doi:10.1016/j.progpolymsci.2013.06.004

Sahoo, T. R., and Prelot, B. (2020). "Adsorption Processes for the Removal of Contaminants from Wastewater," in *Nanomaterials for the Detection and Removal of Wastewater Pollutants* (Elsevier), 161–222. doi:10.1016/B978-0-12-818489-9.00007-4

Salgot, M., and Folch, M. (2018). Wastewater Treatment and Water Reuse. *Curr. Opin. Environ. Sci. Health* 2, 64–74. doi:10.1016/j.coesh.2018.03.005

Saravanane, R., Ranade, V. V., Bhandari, V. M., and Seshagiri Rao, A. (2014). "Urban Wastewater Treatment for Recycling and Reuse in Industrial Applications," in *Industrial Wastewater Treatment, Recycling and Reuse* (Elsevier), 283–322. doi:10.1016/B978-0-08-099968-5.00007-6

Sartape, A. S., Mandhare, A. M., Jadhav, V. V., Raut, P. D., Anuse, M. A., and Kolekar, S. S. (2017). Removal of Malachite green Dye from Aqueous Solution with Adsorption Technique Using Limonia Acidissima (wood Apple) Shell as Low Cost Adsorbent. *Arabian J. Chem.* 10, S3229–S3238. doi:10.1016/j.arabjc.2013.12.019

Say, R., Ersöz, A., Türk, H., and Denizli, A. (2004). Selective Separation and Preconcentration of Cyanide by a Column Packed with Cyanide-Imprinted Polymeric Microbeads. *Sep. Purif. Tech.* 40, 9–14. doi:10.1016/j.seppur.2003.12.021

Seven, F., and Sahiner, N. (2013). Metal Ion-Imprinted Hydrogel with Magnetic Properties and Enhanced Catalytic Performances in Hydrolysis of NaBH4 and NH3BH3. *Int. J. Hydrogen Energ.* 38, 15275–15284. doi:10.1016/j.ijhydene.2013.09.076

S. K. Sharma and R. Sanghi (Editors) (2012). *Advances in Water Treatment and Pollution Prevention* (Dordrecht: Springer Netherlands). doi:10.1007/978-94-007-4204-8

Van Tran, V., Park, D., and Lee, Y.-C. (2018). Hydrogel Applications for Adsorption of Contaminants in Water and Wastewater Treatment. *Environ. Sci. Pollut. Res.* 25, 24569–24599. doi:10.1007/s11356-018-2605-y

Wagner, M., Eicheler, C., Helmreich, B., Hilbig, H., and Heinz, D. (2020). Removal of Congo Red from Aqueous Solutions at Hardened Cement Paste Surfaces. *Front. Mater.* 7. doi:10.3389/fmats.2020.567130

Wei, J., Liu, X., and Xu, S. (2016). Adsorption Behaviors of Ammonium Nitrogen by an Amphoteric Hydrogel. *Desalination Water Treat.* 57, 5753–5759. doi:10.1080/19443994.2014.1003605

Yadav, S. K., Dhakate, S. R., and Pratap Singh, B. (2022). Carbon Nanotube Incorporated eucalyptus Derived Activated Carbon-Based Novel Adsorbent for Efficient Removal of Methylene Blue and Eosin Yellow Dyes. *Bioresour. Tech.* 344, 126231. doi:10.1016/j.biortech.2021.126231

Yildiz, S., Aktas, N., and Sahiner, N. (2014). Metal Nanoparticle-Embedded Super Porous Poly(3-Sulfopropyl Methacrylate) Cryogel for H$_2$ Production from Chemical Hydride Hydrolysis. *Int. J. Hydrogen Energ.* 39, 14690–14700. doi:10.1016/j.ijhydene.2014.07.035

Zhang, X., Elsayed, I., Navarathna, C., Schueneman, G. T., and Hassan, E. B. (2019). Biohybrid Hydrogel and Aerogel from Self-Assembled Nanocellulose and Nanochitin as a High-Efficiency Adsorbent for Water Purification. *ACS Appl. Mater. Inter.* 11, 46714–46725. doi:10.1021/acsami.9b15139